

## Dynamic analysis of the high-power factor three-phase AC to DC converter using current injection hybrid resonant technique

Rahimi Baharom, Mohammad Nawawi Seroji

Faculty of Electrical Engineering, Universiti Teknologi MARA, Malaysia

---

### Article Info

#### Article history:

Received Jun 12, 2018

Revised Nov 29, 2018

Accepted Dec 14, 2018

---

#### Keywords:

AC-DC converter

Current injection technique

Dynamic analysis

Hybrid resonant converter

---

### ABSTRACT

This paper presents the dynamic analysis of the high-power factor three-phase ac to dc converter using current injection hybrid resonant technique in order to investigate the characteristics of the output voltage, line current, DC-link voltage and the resonant current of the proposed converter. The dynamic analysis has been developed based on a separate analysis of the rectifier line-frequency operation and at the resonant circuit high-frequency. Converter circuit analysis has been performed based on the operation at the fundamental frequency. The power balance relation method has been included in order to match the line frequency equation with the high frequency resonant stage equation. This analysis can be envisaged to be the heart of the small-signal model to design the output voltage regulation and maintain a high-power factor input line current of the proposed converter.

Copyright © 2019 Institute of Advanced Engineering and Science.  
All rights reserved.

---

### Corresponding Author:

Rahimi Baharom,  
Faculty of Electrical Engineering,  
Universiti Teknologi MARA,  
40450 Shah Alam, Selangor, Malaysia.  
Email: rahimi6579@gmail.com

---

## 1. INTRODUCTION

The existing research work is mainly concerned the investigation of three-phase AC-DC CIHRC topology to achieve a high power factor and low device stresses by injecting high switching frequency current into the midpoint of the three-phase bridge rectifier combined with the input line frequency current resulting in high-frequency modulation at the midpoint of the diodes. The current injection technique was adopted due to its suitability in applications of AC-DC converter topologies besides its high performance in terms of power factor, efficiency, reliability, light in weight, output voltage regulation and simple upgrading to the existing three-phase AC-DC converters [1], [2]. In addition to that, the current injection technique was more practical due to its simplicity [3]. By using the hybrid resonant configuration, the resonant current dependency problem of the series circuit configuration can be solved, allowing the control of the output voltage at no-load or small load conditions. Moreover, the use of high switching frequency will in theory lead to small element values of the resonant tank and hence improving the power density of the converter topology.

In this research paper, dynamic analysis of the three-phase AC-DC CIHRC has been developed. This novel analysis have been derived based on the steady-state circuit analysis as developed in [4], [5] to improve the understanding of the behaviour of the circuit topology in terms of its controllability, stability and sustainability. Furthermore, the developed dynamic analysis can provide accurate prediction of the output voltage transients of the converter circuit topology. Thus, this analysis can be used to form the basis for the small-signal model to design the closed-loop voltage controller in order to regulate the output voltage of the converter whilst at the same time also it can function to correct the pulsating nature of the supply current to almost unity power factor with a low total harmonic distortion (THD) level well below the acceptable limit that is defined in the standards of IEEE Std. 519 and maintaining the high quality input line current. This was

implemented using an appropriate design of the hybrid resonant circuit with a suitable switching frequency selection that could enable the devices to operate under virtually lossless zero voltage switching (ZVS) conditions.

## 2. THREE-PHASE AC TO DC WITH CURRENT INJECTION HYBRID RESONANT TECHNIQUE

The circuit structure of the three-phase AC to DC using current injection hybrid resonant technique is presented in the Figure 1 which consists of a single, high-frequency inverter leg that operates from the split-capacitor DC-link where the transistor duty ratios were fixed at 0.5. The autotransformer  $T_A$  steps up the output voltage from the switching leg and drove a sinusoidal current through the hybrid resonant circuit. The resonant current was rectified to form the output and was also injected into the three-phase utility-frequency rectifier to modulate the rectifier input voltages resulting in continuous and sinusoidal line currents. The inclusion of capacitor  $C_{PA}$  at the input of the high frequency full-wave rectifier is the main difference with the series circuit topology, thus, make this circuit topology operate as hybrid resonant converter.

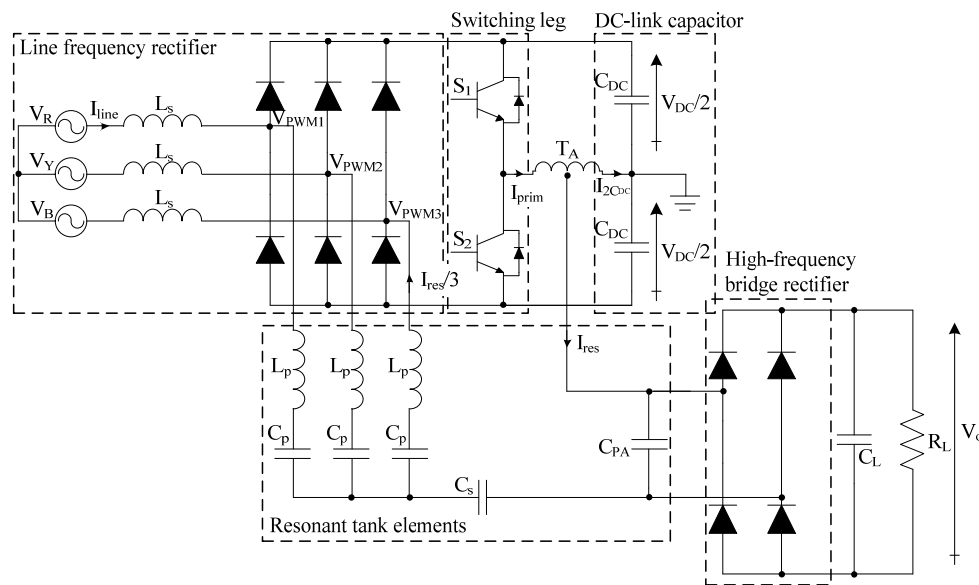


Figure 1. The three-phase AC-DC current injection hybrid resonant converter topology

## 3. DYNAMIC ANALYSIS OF THREE-PHASE AC TO DC CONVERTER USING CURRENT INJECTION HYBRID RESONANT TECHNIQUE

This section describes the derivation of a dynamic analysis for the three-phase AC to DC using current injection hybrid resonant technique. The dynamic analysis for the CIHRC was done by considering that the converter would involve two stages:

- The line-frequency rectifier
- High-frequency resonant circuit

The analysis of line-frequency of the three-phase PWM AC to DC converter was based on the standard method as discussed in [6]. The resulting circuit equations that were expressed in state-space form were then averaged to remove the ripple. After that, the direct and quadrature (d-q) transformation method was adopted to eliminate the time variance in the equations. In order to model the high-frequency resonant stage, the fundamental frequency methods as discussed in [7] were adopted. To match the line frequency equations of the three-phase PWM AC-DC converter with the high-frequency resonant stage equations, the power balanced relations for the DC link methods were employed.

### 3.1. Line frequency rectifier

Figure 2 shows the simplified diagram of the line-frequency rectifier. The total DC-link voltage  $V_{DC}$  was obtained from a series connected of the two split DC link capacitors represented by the DC link

capacitor,  $C_{DC}$ . The line currents and supply voltages were represented by  $i_i$  and  $V_i$  respectively, where  $i$  represents the 1, 2 and 3 phases. The line inductance and its small resistance were represented by  $L_s$  and  $R_s$  respectively. The three-phase diode bridge rectifier were denoted by  $D_j$ , where  $j=1\dots6$ . The switching function of each diodes leg were represented by  $S_i$  where  $i$  is one '1' when the upper diode of the leg is conducting while  $i$  is zero '0' when the lower diode is conducting.

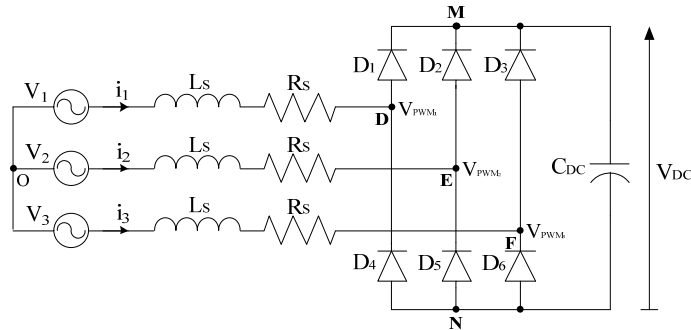


Figure 2. A simplified of the line frequency AC-DC converter

Based on the circuit configuration shown in Figure 1, the phase voltage equation can be derived by applying the Kirchoff's voltage law, resulting in:

$$v_1 = i_1 R_s + L_s \frac{di_1}{dt} + v_{DN} + v_{NO} \quad (1)$$

where  $R_s$  is the series resistance of the line inductor.  $v_{DN}$  is the input voltage of the first leg at point D, with respects to the negative point, N of the DC-link.  $v_{NO}$  is the voltage between point N and the star point of the input supply voltage. By considering the switching function notation of  $v_{DN} = V_{DC}S_1$ , where  $S_1$  is a function of conducting of diode  $D_1$ , thus, (1) can be simplified as:

$$v_1 = i_1 R_s + L_s \frac{di_1}{dt} + V_{DC}S_1 + v_{NO} \quad (2)$$

The method for derive the first phase equation can be applied to solve phases 2 and 3. Therefore, the phase 2 and phase 3 equations can be derived as;

$$v_2 = i_2 R_s + L_s \frac{di_2}{dt} + V_{DC}S_2 + v_{NO} \quad (3)$$

$$v_3 = i_3 R_s + L_s \frac{di_3}{dt} + V_{DC}S_3 + v_{NO} \quad (4)$$

For a three-phase system without a neutral line,

$$i_1 + i_2 + i_3 = 0 \quad (5)$$

By assuming that the three-phase AC supply voltages were balanced, the summation of the instantaneous voltages will be equal to zero.

$$v_1 + v_2 + v_3 = 0 \quad (6)$$

Rearranging (2), (3) and (4) will result in;

$$i_1 = - \left[ \frac{L_s \frac{di_1}{dt} + V_{DC}S_1 + v_{NO} - v_1}{R_s} \right]$$

$$i_2 = - \left[ \frac{L_s \frac{di_2}{dt} + V_{DC} S_2 + v_{NO} - v_2}{R_s} \right]$$

$$i_3 = - \left[ \frac{L_s \frac{di_3}{dt} + V_{DC} S_3 + v_{NO} - v_3}{R_s} \right]$$

Substituting the above into (5), hence;

$$v_{NO} = -\frac{1}{3} V_{DC} \sum_1^3 S_k \quad (7)$$

The input side of the converter can be obtained by substituting (7) into (2), (3) and (4) represented by the following:

$$L_s \dot{i}_1 = -R_s i_1 - \left( S_1 - \frac{1}{3} \sum_1^3 S_k \right) V_{DC} + v_1 \quad (8)$$

$$L_s \dot{i}_2 = -R_s i_2 - \left( S_2 - \frac{1}{3} \sum_1^3 S_k \right) V_{DC} + v_2 \quad (9)$$

$$L_s \dot{i}_3 = -R_s i_3 - \left( S_3 - \frac{1}{3} \sum_1^3 S_k \right) V_{DC} + v_3 \quad (10)$$

or in the matrix form as:

$$\mathbf{Z}\dot{\mathbf{x}} = \mathbf{A}\mathbf{x} + \mathbf{e} \quad (11)$$

Here:

$$\mathbf{x} = \begin{bmatrix} i_1 \\ i_2 \\ i_3 \end{bmatrix}$$

$$\mathbf{A} = \begin{bmatrix} -R_s & 0 & 0 \\ 0 & -R_s & 0 \\ 0 & 0 & -R_s \end{bmatrix}$$

$$\mathbf{Z} = \begin{bmatrix} L_s & 0 & 0 \\ 0 & L_s & 0 \\ 0 & 0 & L_s \end{bmatrix}$$

$$\mathbf{e} = \begin{bmatrix} - \left( S_1 - \frac{1}{3} \sum_1^3 S_k \right) V_{DC} + v_1 \\ - \left( S_2 - \frac{1}{3} \sum_1^3 S_k \right) V_{DC} + v_2 \\ - \left( S_3 - \frac{1}{3} \sum_1^3 S_k \right) V_{DC} + v_3 \end{bmatrix}$$

The circuit (11) can be simplified by averaging the switching functions, hence removing the high frequency information [8]. Furthermore, by employing the transformation to a rotating reference frame, the supply frequency time variance can be removed.

### 3.1.1. Averaging procedure

For a natural sampling sinusoidal pulse-width modulation, the switching points within one switching period are not symmetrical. However, when the switching frequency is much higher than the line frequency,

the modulating wave can be regarded as a constant within each switching period. Therefore, the switching pattern is close to be symmetrical [9]. In this way, the local average value or duty ratio  $\bar{S}_i$  can be used to replace the switching function  $S_i$  in any specific period. The use of current injection sinusoidal PWM scheme resulting in the supply current that is in phase with the fundamental of the PWM voltage,  $V_{PWM1}$ . The  $V_{PWM1}$  is lagging the supply voltage,  $V_s$  by an angle  $\phi$  as shown in Figure 3, with the assumption that the phase angle was unaffected with the small resistance  $R_s$ .

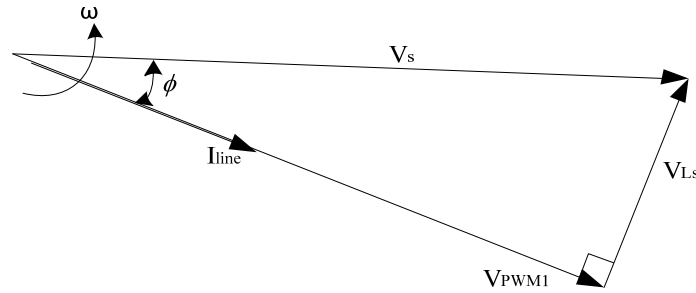


Figure 3. Fundamental frequency phasor diagram

By referring to the phasor diagram shown in Figure 2 and by using the relationship in (2), it can be seen that the fundamental of the PWM voltage of phase  $i=R,Y,B$  where  $R=1, Y=2$  and  $B=3$  can be expressed as;

$$V_{PWM1i} = \frac{V_{DC}}{2} f_f(M) \sin \left( (\omega t - \phi) - (i - 1) \frac{2\pi}{3} \right) \quad (12)$$

And for phase  $i$ ,

$$L_s \dot{i}_1 = -i_1 R_s - V_{PWM1i} + v_i \quad (13)$$

Therefore, the local average switching function  $\bar{S}_i$  in matrix  $e$  could be obtained by comparing (13) with (11). Thus, the resulting equation can be expressed as:

$$\bar{S}_i - \frac{1}{3} \sum_1^3 \bar{S}_k = \frac{f_f(M)}{2} \sin \left[ (\omega t - \phi) - (i - 1) \frac{2\pi}{3} \right] \quad (14)$$

Finally, the matrix  $e$  in (11) can be simplified as follows:

$$e = \begin{bmatrix} -V_{DC} \frac{f_f(M)}{2} \sin(\omega t - \phi) + v_1 \\ -V_{DC} \frac{f_f(M)}{2} \sin \left[ (\omega t - \phi) - \frac{2\pi}{3} \right] + v_2 \\ -V_{DC} \frac{f_f(M)}{2} \sin \left[ (\omega t - \phi) - \frac{4\pi}{3} \right] + v_3 \end{bmatrix} \quad (15)$$

### 3.1.2. Elimination of the time-variance

The transformation to a rotating reference frame technique was adopted to eliminate the time-varying switching function in (11) and used to further simplify the model. In this way, three-phase quantities were transformed to direct and quadrature axis (d-q) components using the transformation matrix,  $T^{-1}$ . Then, the d-q quantities were transformed back to their three-phase quantities using the inverse matrix  $T$ . This process is known as the non-power invariant Park transformation [8]. Therefore, the transformation matrix  $T^{-1}$  can be expressed as;

$$\mathbf{T}^{-1} = \frac{2}{3} \begin{bmatrix} \cos \omega t & \cos \left( \omega t - \frac{2\pi}{3} \right) & \cos \left( \omega t - \frac{4\pi}{3} \right) \\ -\sin \omega t & -\sin \left( \omega t - \frac{2\pi}{3} \right) & -\sin \left( \omega t - \frac{4\pi}{3} \right) \\ \frac{1}{2} & \frac{1}{2} & \frac{1}{2} \end{bmatrix} \quad (16)$$

Meanwhile, the inverse matrix  $\mathbf{T}$  is given by:

$$\mathbf{T} = \begin{bmatrix} \cos \omega t & -\sin \omega t & 1 \\ \cos \left( \omega t - \frac{2\pi}{3} \right) & -\sin \left( \omega t - \frac{2\pi}{3} \right) & 1 \\ \cos \left( \omega t - \frac{4\pi}{3} \right) & -\sin \left( \omega t - \frac{4\pi}{3} \right) & 1 \end{bmatrix} \quad (17)$$

The relationship between the vector  $\mathbf{x}$  in the stationary frame and the new state vector  $\mathbf{x}_r$  in the rotating frame can be expressed as follows:

$$\mathbf{x}_r = [i_D \quad i_Q \quad i_0]^T = \mathbf{T}^{-1} \mathbf{x} \quad (18)$$

The original state vector alternatively can be expressed as:

$$\mathbf{x} = \mathbf{T} \mathbf{x}_r \quad (19)$$

where the d, q, and zero sequence components of the line currents are represented by  $i_D$ ,  $i_Q$  and  $i_0$  respectively. Differentiating (19) gives:

$$\dot{\mathbf{x}} = \mathbf{T} \dot{\mathbf{x}}_r + \dot{\mathbf{T}} \mathbf{x}_r \quad (20)$$

By substituting (19) and (20) into (11), yielding:

$$\mathbf{Z}(\mathbf{T} \dot{\mathbf{x}}_r + \dot{\mathbf{T}} \mathbf{x}_r) = \mathbf{A}(\mathbf{T} \mathbf{x}_r) + \mathbf{e} \quad (21)$$

Multiplying out and rearranging (21) resulting in:

$$\mathbf{ZT} \dot{\mathbf{x}}_r = (\mathbf{AT} - \mathbf{Z}\dot{\mathbf{T}}) \mathbf{x}_r + \mathbf{e} \quad (22)$$

By using  $\mathbf{ZT} = \mathbf{TZ}$  as follows, which gives:

$$\mathbf{TZ} \dot{\mathbf{x}}_r = (\mathbf{AT} - \mathbf{Z}\dot{\mathbf{T}}) \mathbf{x}_r + \mathbf{e} \quad (23)$$

Therefore,

$$\mathbf{Z} \dot{\mathbf{x}}_r = \mathbf{T}^{-1}(\mathbf{AT} - \mathbf{Z}\dot{\mathbf{T}}) \mathbf{x}_r + \mathbf{T}^{-1} \mathbf{e} \quad (24)$$

Where,  $\mathbf{T}^{-1}(\mathbf{AT} - \mathbf{Z}\dot{\mathbf{T}})$  is;

$$\mathbf{T}^{-1}(\mathbf{AT} - \mathbf{Z}\dot{\mathbf{T}}) = \begin{bmatrix} -R_s & \omega L_s & 0 \\ -\omega L_s & -R_s & 0 \\ 0 & 0 & -R_s \end{bmatrix} \quad (25)$$

and from (25),  $\mathbf{T}^{-1} \mathbf{e}$  can be separated into:

$$\mathbf{T}^{-1} \mathbf{e} = \mathbf{T}^{-1} \begin{bmatrix} -V_{DC} \frac{f_f(M)}{2} \sin(\omega t - \phi) \\ -V_{DC} \frac{f_f(M)}{2} \sin \left( (\omega t - \phi) - \frac{2\pi}{3} \right) \\ -V_{DC} \frac{f_f(M)}{2} \sin \left( (\omega t - \phi) - \frac{4\pi}{3} \right) \end{bmatrix} + \mathbf{T}^{-1} \begin{bmatrix} V_1 \\ V_2 \\ V_3 \end{bmatrix} \quad (26)$$

Therefore;

$$\mathbf{T}^{-1} \begin{bmatrix} -V_{DC} \frac{f_f(M)}{2} \sin(\omega t - \phi) \\ -V_{DC} \frac{f_f(M)}{2} \sin\left((\omega t - \phi) - \frac{2\pi}{3}\right) \\ -V_{DC} \frac{f_f(M)}{2} \sin\left((\omega t - \phi) - \frac{4\pi}{3}\right) \end{bmatrix} = \begin{bmatrix} V_{DC} \frac{f_f(M)}{2} \sin \phi \\ V_{DC} \frac{f_f(M)}{2} \cos \phi \\ 0 \end{bmatrix} \quad (27)$$

Assuming that the d-q transformation of the three-phase supply voltage yields:

$$\mathbf{T}^{-1} \begin{bmatrix} v_1 \\ v_2 \\ v_3 \end{bmatrix} = \begin{bmatrix} V_D \\ V_Q \\ 0 \end{bmatrix} \quad (28)$$

where  $V_D$  and  $V_Q$  are the d and q components of the three-phase supply voltages  $v_1$ ,  $v_2$ , and  $v_3$ . By substituting (25), (26), (27) and (28) into (24), the three-phase line frequency rectifier can be represented by the following set of time-invariant, state-space equations in a rotating frame as the reference:

$$\begin{bmatrix} L_s & 0 & 0 \\ 0 & L_s & 0 \\ 0 & 0 & L_s \end{bmatrix} \begin{bmatrix} \dot{i}_D \\ \dot{i}_Q \\ \dot{i}_0 \end{bmatrix} = \begin{bmatrix} -R_s & \omega L_s & 0 \\ -\omega L_s & -R_s & 0 \\ 0 & 0 & -R_s \end{bmatrix} \begin{bmatrix} i_D \\ i_Q \\ i_0 \end{bmatrix} + \begin{bmatrix} \frac{V_{DC}}{2} f_f(M) \sin \phi + V_D \\ \frac{V_{DC}}{2} f_f(M) \cos \phi + V_Q \\ 0 \end{bmatrix} \quad (29)$$

By neglecting the neutral line in the symmetrical three-phase system, the zero sequence component  $i_0$  can be ignored. By using the transformation to a rotating reference frame method, the d-axis is  $90^\circ$  ahead of the phasor of the supply voltage, resulting in  $V_D = 0$  and  $V_Q = -\sqrt{2}V_s$ . As a result of this, the time variant equations can be expressed by multiplying out (29) to be.

$$L_s \dot{i}_D = -R_s i_D + \omega L_s i_Q + \frac{V_{DC}}{2} f_f(M) \sin \phi \quad (30)$$

$$L_s \dot{i}_Q = -\omega L_s i_D - R_s i_Q + \frac{V_{DC}}{2} f_f(M) \cos \phi - \sqrt{2}V_s \quad (31)$$

$\sin \phi$  can be obtained from the fundamental frequency phasor diagram in Figure 3.

$$\sin \phi = \frac{V_{L_s}}{V_s} = \frac{I_{line} X_{L_s}}{V_s} \quad (32)$$

The d-q transformation of the line current gives:

$$I_{line} = \frac{\sqrt{i_D^2 + i_Q^2}}{\sqrt{2}} = \sqrt{\frac{1}{2}(i_D^2 + i_Q^2)} \quad (33)$$

$$i_Q = \frac{i_D}{\tan \phi}$$

Therefore,

$$\sqrt{2}I_{line} = \sqrt{i_D^2 + \frac{i_D^2}{\tan^2 \phi}}$$

$$\sqrt{2}I_{line} = i_D \sqrt{1 + \frac{1}{\tan^2 \phi}}$$

As a result of;

$$i_D = i_{line} \sqrt{\frac{2 \tan \phi^2}{1 + \tan \phi}}$$

Finally, the resonant current can be derived as:

$$I_{res} = \frac{3I_{line}}{M} \quad (34)$$

### 3.2. High-frequency resonant stage

Based on the fundamental frequency approximation as discussed in [4], the high-frequency resonant stage was obtained by assuming that the resonant circuit responded immediately to the small-signal changes. Under transient conditions, the difference between the total active power flowing into the DC-link through the three-phase rectifier and the power drawn through the transistor switching leg must flow into or out of the DC-link capacitor. This is the dynamic version of the steady-state power balance in (15), where it was assumed that the difference in power was zero [8]. Therefore;

$$3V_{PWM1}I_{line} + V_{PVMC}I_{res} - \frac{2NV_{DC}}{\sqrt{2}\pi} I_{res} \cos \theta_{DC-DC} = V_{DC}C_{DC} \frac{dV_{DC}}{dt} \quad (35)$$

By using  $\theta_{DC-DC}$  in [5] to eliminate the  $\theta_{DC-DC}$  terms in (35), it will result in:

$$3V_{PWM1}I_{line} + V_{PVMC}I_{res} - \frac{2NV_{DC}I_{res}}{\sqrt{2}\pi} \left[ \frac{\left(\frac{V_o^2}{R_L} + V_{PVMC}I_{res}\right)\sqrt{2}\pi}{2NV_{DC}I_{res}} \right] = V_{DC}C_{DC} \frac{dV_{DC}}{dt}$$

$$3V_{PWM1}I_{line} - \frac{V_o^2}{R_L} = V_{DC}C_{DC} \frac{dV_{DC}}{dt} \quad (36)$$

where;

$$V_{PVM1} = \frac{V_{DC}}{2\sqrt{2}} f_f(M)$$

By substituting  $V_{PVM1}$  into (36), yields;

$$C_{DC} \frac{dV_{DC}}{dt} = \frac{3f_f(M)I_{line}}{2\sqrt{2}} - \frac{V_o^2}{V_{DC}R_L} \quad (37)$$

In order to eliminate the  $\cos \theta_{DC-DC}$  term from [5] yielding;

$$\frac{\left(\frac{V_o^2}{R_L} + V_{PVMC}I_{res}\right)\sqrt{2}\pi}{2NV_{DC}I_{res}} = \frac{\left(\frac{V_{PVMC}}{V_{DC}}\right)^2 + \left(\frac{2N}{\sqrt{2}\pi}\right)^2 - \left(\frac{I_{res}Z_{res}}{V_{DC}}\right)^2}{\frac{4N}{\sqrt{2}\pi} \left(\frac{V_{PVMC}}{V_{DC}}\right)}$$

$$(I_{res}Z_{res})^2 + \frac{[V_{DC}f_c(M)]^2}{8} + \frac{V_o^2 V_{DC} f_c(M)}{\sqrt{2} I_{res} R_L} - 2 \left(\frac{NV_{DC}}{\pi}\right)^2 = 0 \quad (38)$$

In order to complete the model of the converter, the dynamic relationship between the output voltage,  $V_o$  and the output current,  $I_o$  was required.  $I_o$  is the local average of the rectified bridge current,  $I_B$  that was fed into the parallel combination of the load resistor and filter capacitor as illustrated in Figure 4 and Figure 5.  $I_z$  is the small current disturbance placed in parallel with the load resistor  $R_L$  and is an analytical tool to examine the load current changes. The differential equation for the output filter capacitor,  $C_o$  can be expressed as:

$$I_o - I_z = \frac{V_o}{R_L} + C_o \frac{dV_o}{dt} \quad (39)$$

where,

$$C_o \frac{dV_o}{dt} = I_o - I_z - \frac{V_o}{R_L}$$

$$I_{res} = I_{C_{PA}} + I_B$$

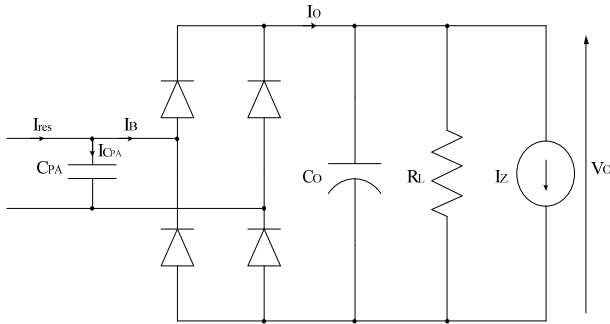


Figure 4. Output rectifier unit under dynamic conditions

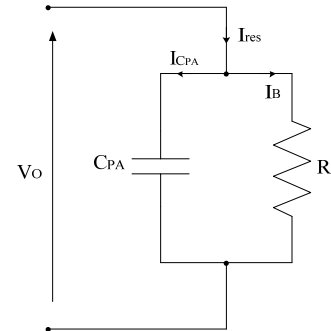


Figure 5. Current flow through output rectifier unit under transient conditions

So,

$$I_o = \frac{2}{\pi} \sqrt{2} I_B$$

$$I_B = I_{res} - I_{C_{PA}}$$

$$I_{C_{PA}} = C_{PA} \frac{dV_o}{dt}$$

Hence,

$$I_o = \frac{2}{\pi} \sqrt{2} \left( I_{res} - C_{PA} \frac{dV_o}{dt} \right) \tag{40}$$

Where,

$$V_o = I_{res} R_T \tag{41}$$

Substitute (41) into (39), resulting in;

$$\frac{dV_o}{dt} = \frac{\frac{2}{\pi} \sqrt{2} I_{res} - I_z - \frac{V_o}{R_L}}{C_o + \frac{2\sqrt{2} C_{PA}}{\pi}} \tag{42}$$

and function  $v$  represents the right hand side of (42).

#### 4. CONCLUSION

In this paper, a dynamic analysis of the three-phase AC to DC converter using current injection hybrid resonant technique was derived. In general, it the design of dynamic analysis was to provide an accurate prediction of the output voltage, line current, DC-link voltage and resonant current transients respond. This mathematical model can be used to develop a small-signal model to design a closed loop controller to regulate the DC output voltage, whilst at the same time also being capable to perform the power factor corrector operation.

**ACKNOWLEDGEMENTS**

Authors gratefully acknowledge the financial support from Institute of Research Management and Innovation (IRMI) Universiti Teknologi MARA Grant No: 600-IRMI/MyRA 5/3/BESTARI (029/2017).

**REFERENCES**

- [1] A. V. T.Chandrasekar, *et al.*, "A Study and Review of Current Injection Techniques, " *International Journal of Technology and Engineering Science [IJTES]*, vol 1, pp. 1008-10013,Sept 2013.
- [2] M. Y. Tarnini, "Harmonic Filtration by Current Injection and Shunt Capacitors Technique," in *2013 3rd International Conference on Electric Power and Energy Conversion Systems (EPECS)*, pp. 1-5, Oct 2013.
- [3] M. Taleb and T. H. Ortmeyer, "Examination of the current injection technique (distribution networks)," in *IEEE Transactions on Power Delivery*, vol. 7, pp. 442-448, Jan. 1992.
- [4] R. Baharom, M. N. Seroji, M. K. M. Salleh and K. S. Muhammad, "A high power factor three-phase AC-DC current injection hybrid resonant converter," *IECON 2016 - 42nd Annual Conference of the IEEE Industrial Electronics Society*, Florence, pp. 3123-3128, 2016.
- [5] R. Baharom *et al.*, "Analysis of Three-Phase AC-DC Current Injection Hybrid Resonant Converter", *Journal of Telecommunication, Electronic and Computer Engineering (JTEC)*, Vol. 9, No.2-7, 2016.
- [6] R. Wu, S. B. Dewan and G. R. Slemon, "A PWM AC to DC converter with fixed switching frequency," *Conference Record of the 1988 IEEE Industry Applications Society Annual Meeting*, Pittsburgh, PA, USA, pp. 706-711 vol.1, 1988.
- [7] R. L. Steigerwald, "High-Frequency Resonant Transistor DC-DC Converters," in *IEEE Transactions on Industrial Electronics*, vol. IE-31, pp. 181-191, May 1984.
- [8] M. N. Seroji, "Analysis and Control Design of a High-Power Factor, Three-Phase AC/DC Converter With High-Frequency Resonant Current Injection, " *Ph.D. dissertation, Department of Electronic, Electrical and Computer Engineering, University of Birmingham*, December 2007.
- [9] R. Wu, S. B. Dewan and G. R. Slemon, "Analysis of an AC-to-DC voltage source converter using PWM with phase and amplitude control," in *IEEE Transactions on Industry Applications*, vol. 27, pp. 355-364, March-April 1991.